SUPPLEMENTAL METHODS

Filtering strategy for WES

Our variant prioritization plan was focused on identifying rare, protein-altering variants consistent with an autosomal recessive inheritance pattern within the regions of interest identified by linkage analysis. We therefore assumed that the causal variant would satisfy the following criteria: the causal variant (1) belongs to the regions of interest identified by linkage analysis (2) segregates perfectly with disease status (3) is either novel or not referenced as a polymorphism (minor allele frequency ≥ 1%) in databases such as dbSNP, 1000 genome projects and an in-house exome sequencing variant database (4) alters a protein's amino-acid sequence, and is likely to disrupt the function of that protein.

The variant identified by exome sequencing was validated by Sanger sequencing, and segregation analysis in the family was verified. Sequence chromatograms were analyzed using the Sequencher software (Gene Codes, Ann Arbor, MI). Positions of mutations were numbered with the A of the ATG-translation initiation codon in the reference cDNA sequence being 1. The functional consequence of each variant was predicted using SIFT (http://sift.jcvi.org/www/SIFT_enst_submit.html) and PolyPhen2 (http://genetics.bwh.harvard.edu/pph2/).

RNA extraction and RT-PCR

Total cellular mRNA was isolated using Qiagen Extraction Kit, then treated with DNase I. 1 µg of total RNA was reverse-transcribed using Superscript II (Life Technologies). Relative expression levels of the *TTC21B* mRNA were determined by real-time RT-PCR using Absolute SYBR Green ROX Mix (ABgene) using specific primers (human *TTC21B* forward: 5'-AGCATGCTCTGGCTCATGAA.-3'; human *TTC21B* reverse: 5'-TTGACAACGTCCATCCTCCAT-3'). *TTC21B* expression performed in triplicate was normalized to *HPRT* mRNA expression. Data were analyzed with the $2^{-\Delta\Delta Ct}$ method.

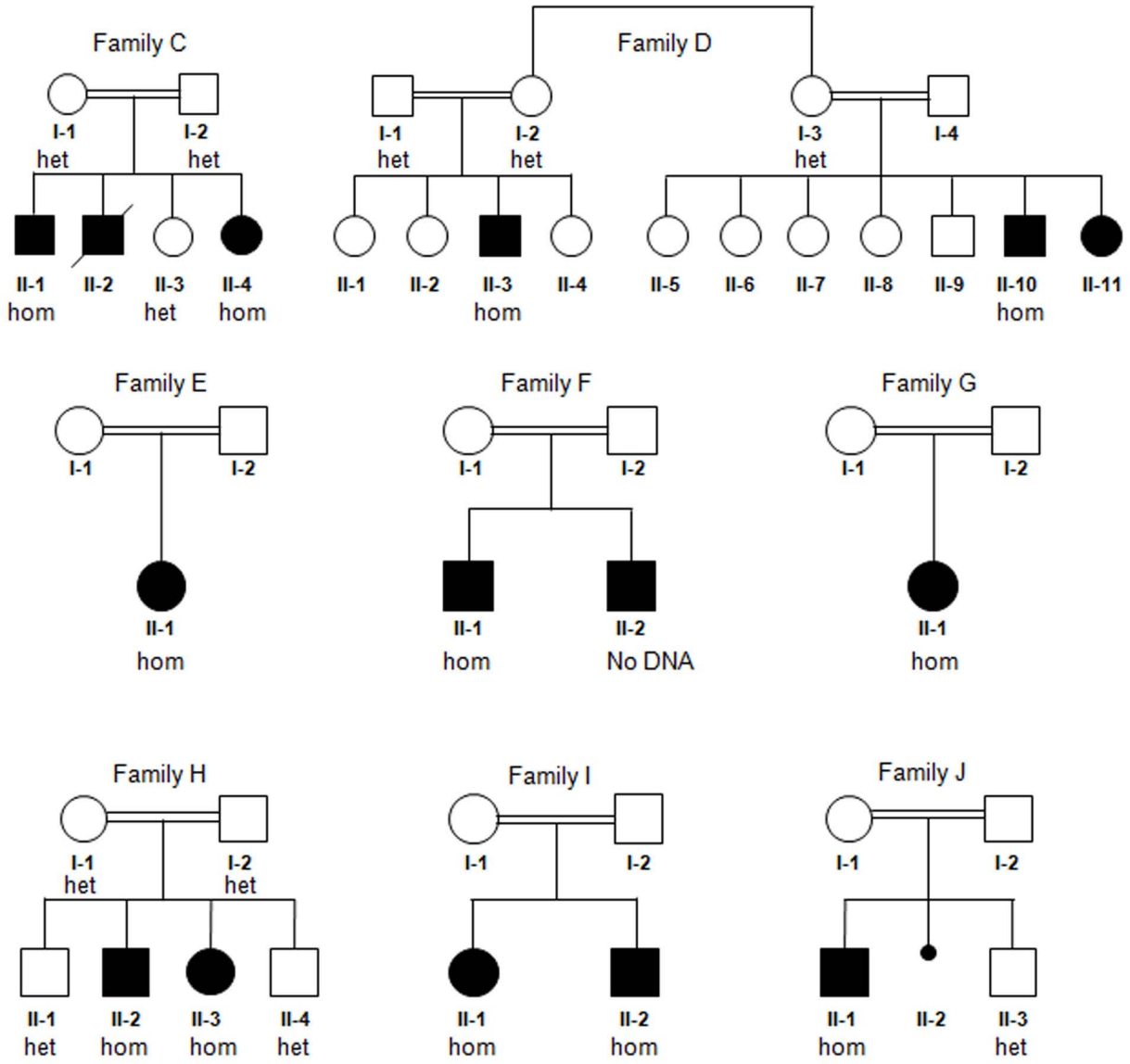

Supplemental Figure 1: Pedigrees of the eight other families (C-J) that carry the homozygous p.P209L mutation. The allele status is given below each tested individual (hom : homozygous, het : heterozygous). Normal individuals are represented by an open square or circle, depending on the sex, and affected individuals by a solid square or circle. Strikethrough represents deceased individual.

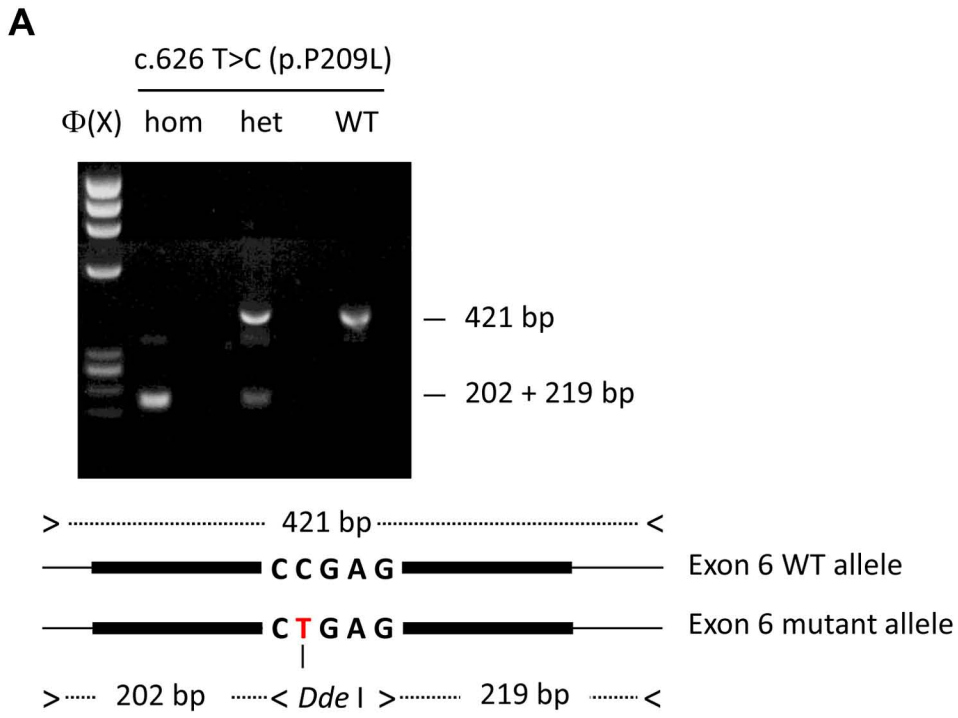

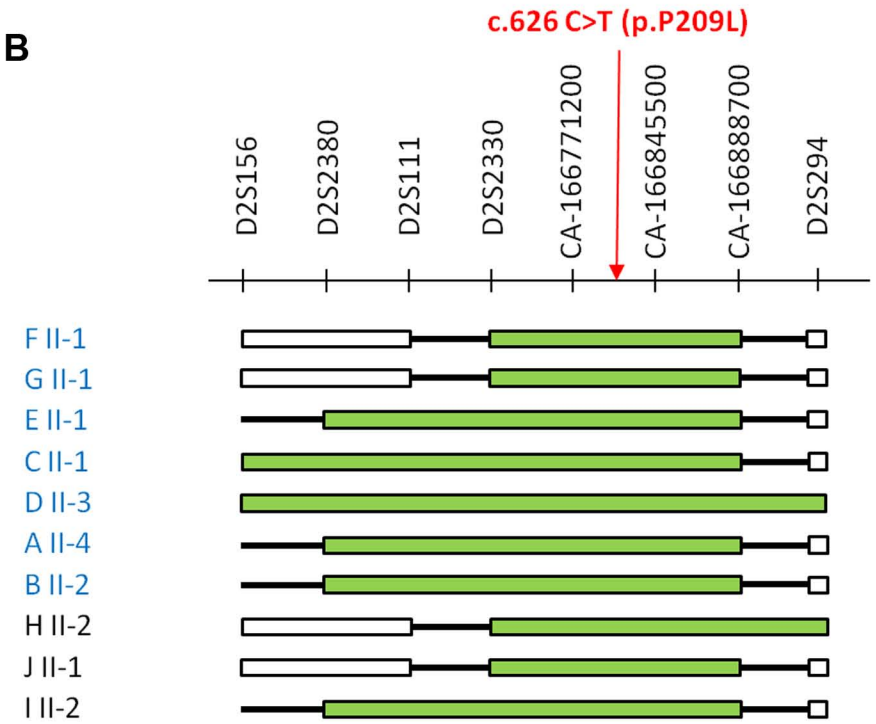

Supplemental Figure 2: (A) *Dde*I digestion of *TTC21B* exon 6 from homozygous (Hom), heterozygous (het) and control indivudals (WT). The mutation creates a *Dde*I site, allowing detection of c.626 T>C (p.P209L) mutation. (B) Haplotype analysis in all index patients homozygous for p.P209L. Eight microsatellite markers spanning 9.7 Mb were tested. A common haplotype (in green) was identified encompassing markers D2S2330 to CA-166888700 with a minimal size of 250 kb.

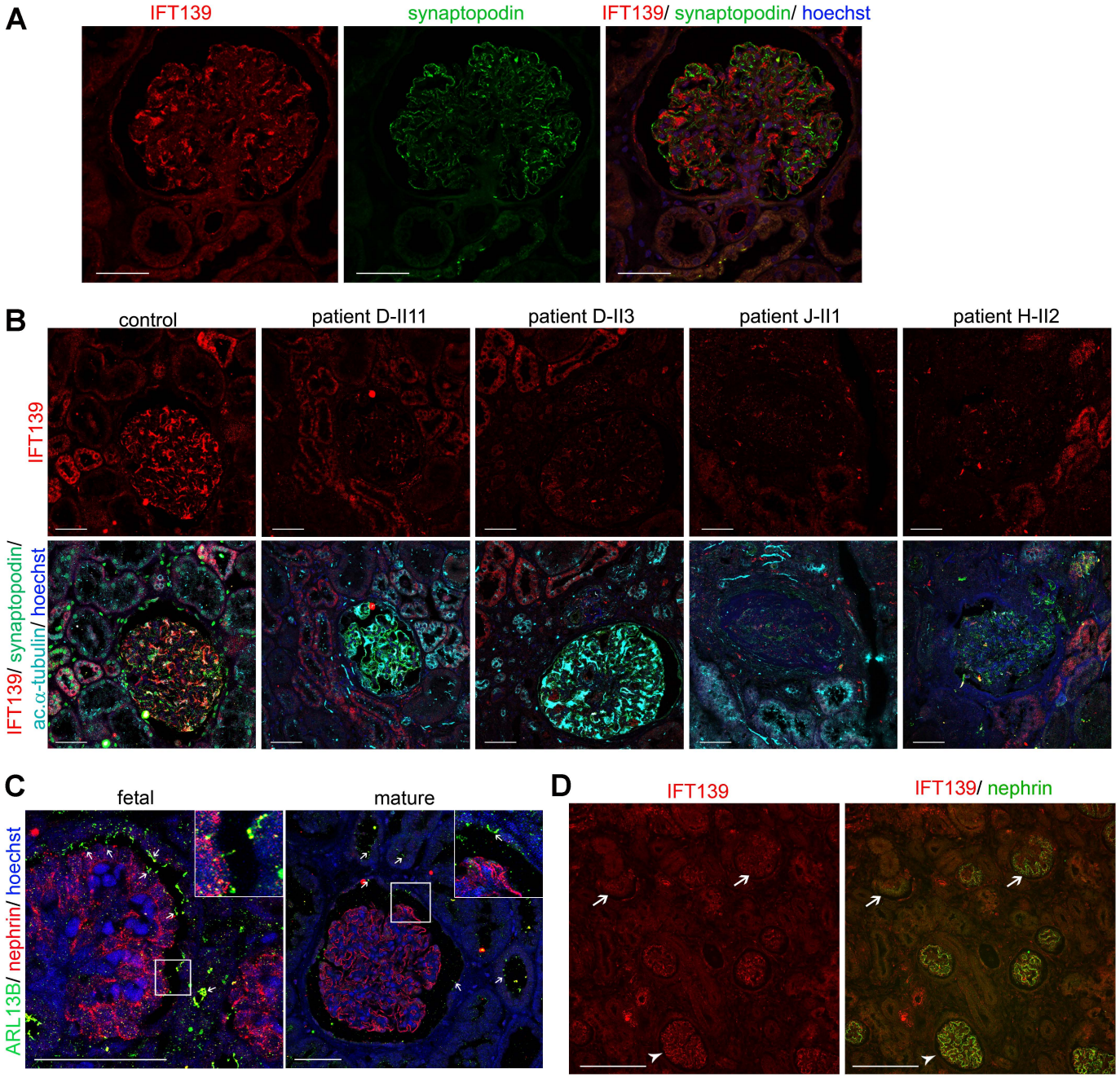

Supplemental Figure 3: (A) Immunolocalization of IFT139 in adult control human kidney using synaptopodin to identify podocytes. IFT139 is expressed in glomerular podocytes. (B) Immunolocalization of IFT139 in adult control and patients kidney. IFT139 staining appears weaker in patients glomeruli compared to control. (C) Immunostaining of ARL13B, a ciliary membrane protein, and nephrin, a podocyte marker, shows presence of cilia (arrows) in developing human podocytes but absence of cilia in mature podocytes. In adult kidney, cilia are only present in tubules and in the Bowman's capsule (arrows). Scale bar: 50 µm. (D) Immnunofluorescence of IFT139 in fetal human kidney (14 weeks old) using nephrin to identify glomeruli. IFT139 expression seems higher in mature (arrow head) compared to developing glomeruli (arrows). Scale bar: 10µm. (E) Expression level of *TTC21B* in differentiated and undifferentiated podocytes by qPCR showed an increase of *TTC21B* mRNA after differentiation. For statistical analysis, three independent experimentations were performed and Student's *t*-test was conducted. The mean +/- SEM is shown (*P<0.05).

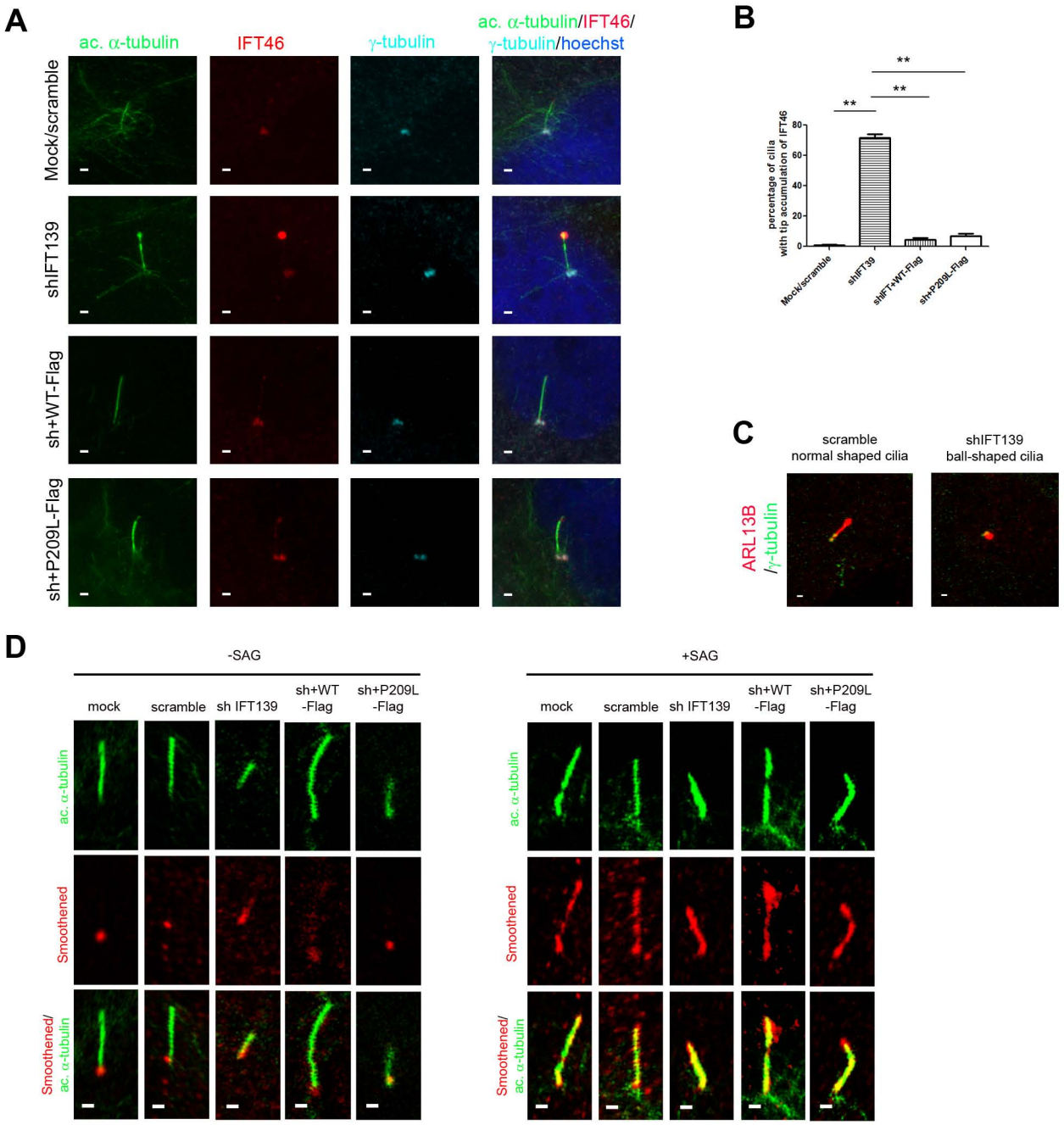

Supplemental Figure 4. (A) Immunolocalization of IFT46 in the primary cilium labelled by acetylated α-tubulin. IFT46 is expressed at the base and in the axoneme of the primary cilium, however the depletion of IFT139 leads to IFT46 accumulation in ciliary tip indicating a defect in retrograde intraflagellar transport. Scale bar : 1µM. (B) Graph representing the quantification of cells harboring tip accumulation at the primary cilium. For statistical analysis, at least three independent experimentations were performed. Student's *t*-test is conducted, the mean ± SEM is shown (*P < 0.05; **P < 0.01). Scale bar : 1µM. (C) Immunolabelling of primary cilium in undifferentiated podocytes using ARL13B illustrates a normal (left panel) and ball-shaped (right panel) cilium. Scale bar : 1µM. (D) Immunolabeling of primary cilia in undifferentiated podocytes using acetylated α-tubulin. In untreated cells, Smoothened localizes at the base of the cilium. Treatment of podocytes with 100nM Smoothened agonist (SAG) for 24 hours induces Smoothened relocalization along the cilium in all cell lines, suggesting that p.P209L does not disrupt the Hedghog pathway. Scale bars: 1µm

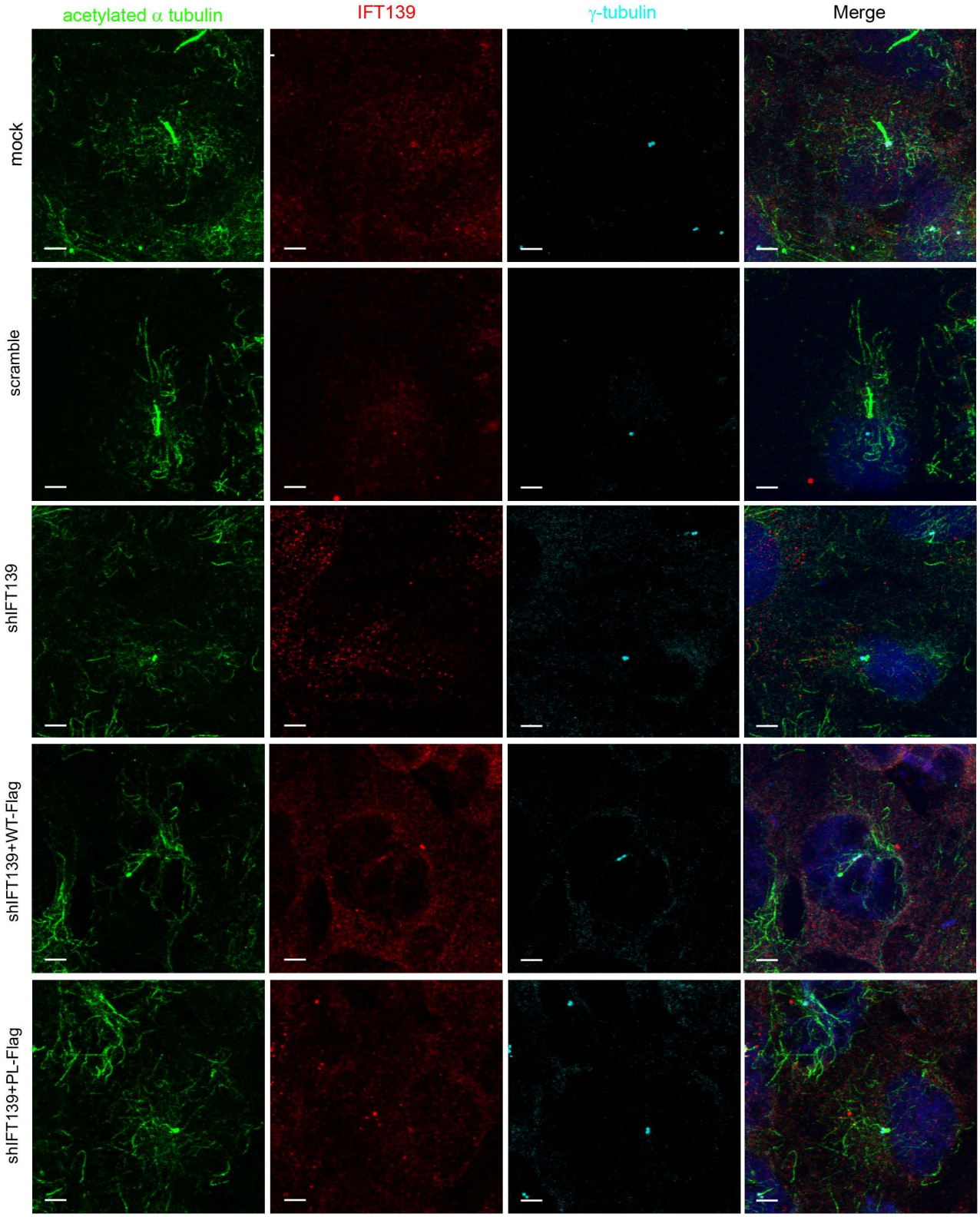

Supplemental figure 5: Acetylated α-tubulin staining shows the cilia as well as an under-developed network of acetylated microtubules. IFT139 labelling confirms its localization at the basal body in ciliated cells, however the cytoplasmic staining is diffuse and IFT139 does not seem to localize along the acetylated microtubule network. Stack images of the whole cell were taken on a LEICA SP8 confocal microscope. Scale bar : 5μM

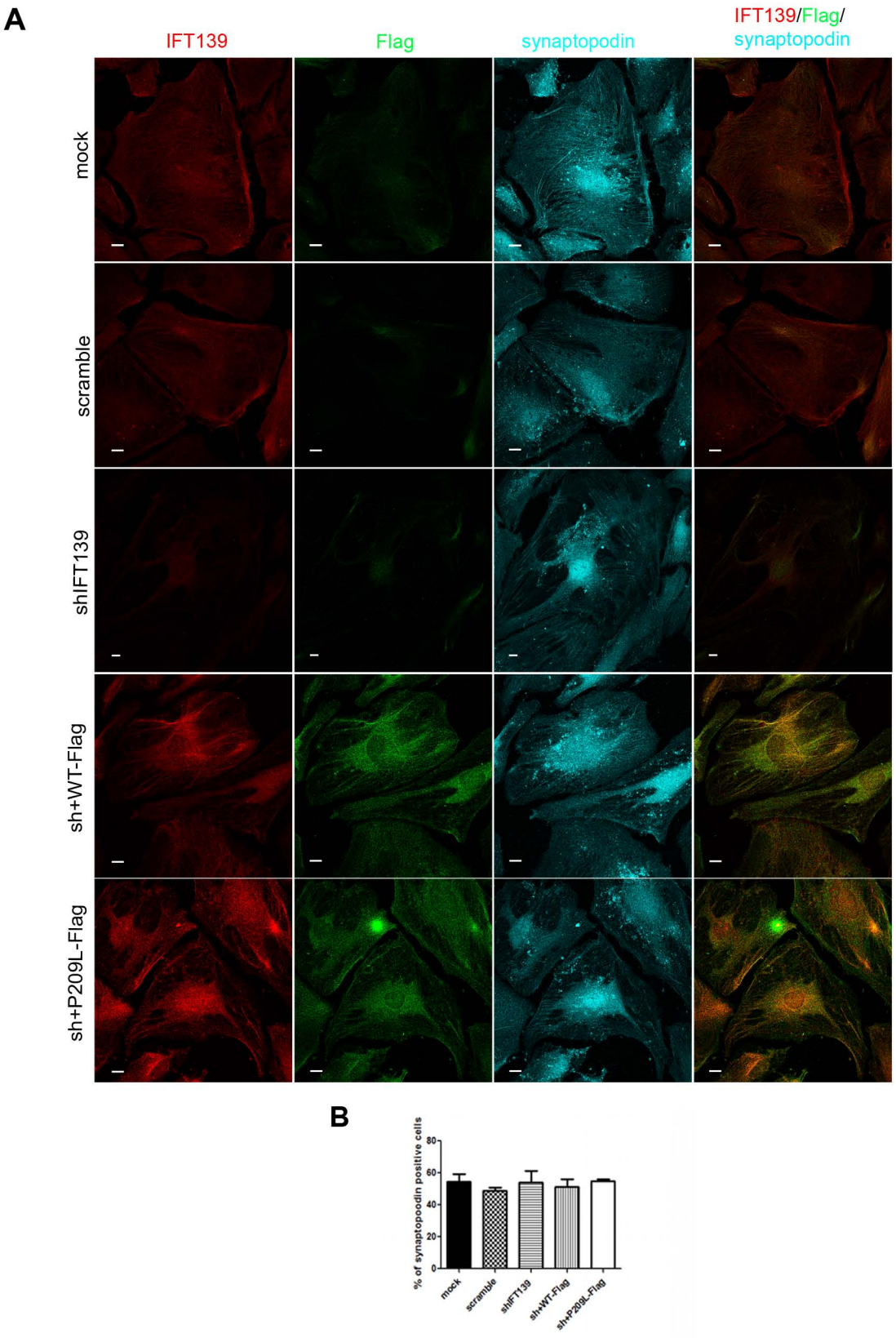

Supplemental Figure 6: (A) IFT139 staining using either IFT139 antibodies or Flag antibodies on differentiated podocytes. Synaptopodin was used to label differentiated cells. Scale bars: 20µm. (B) Graph showing the percentage of differentiated cells. p.P209L expressing cells undergo differentiation. All cell types undergo differentiation at the same rate.

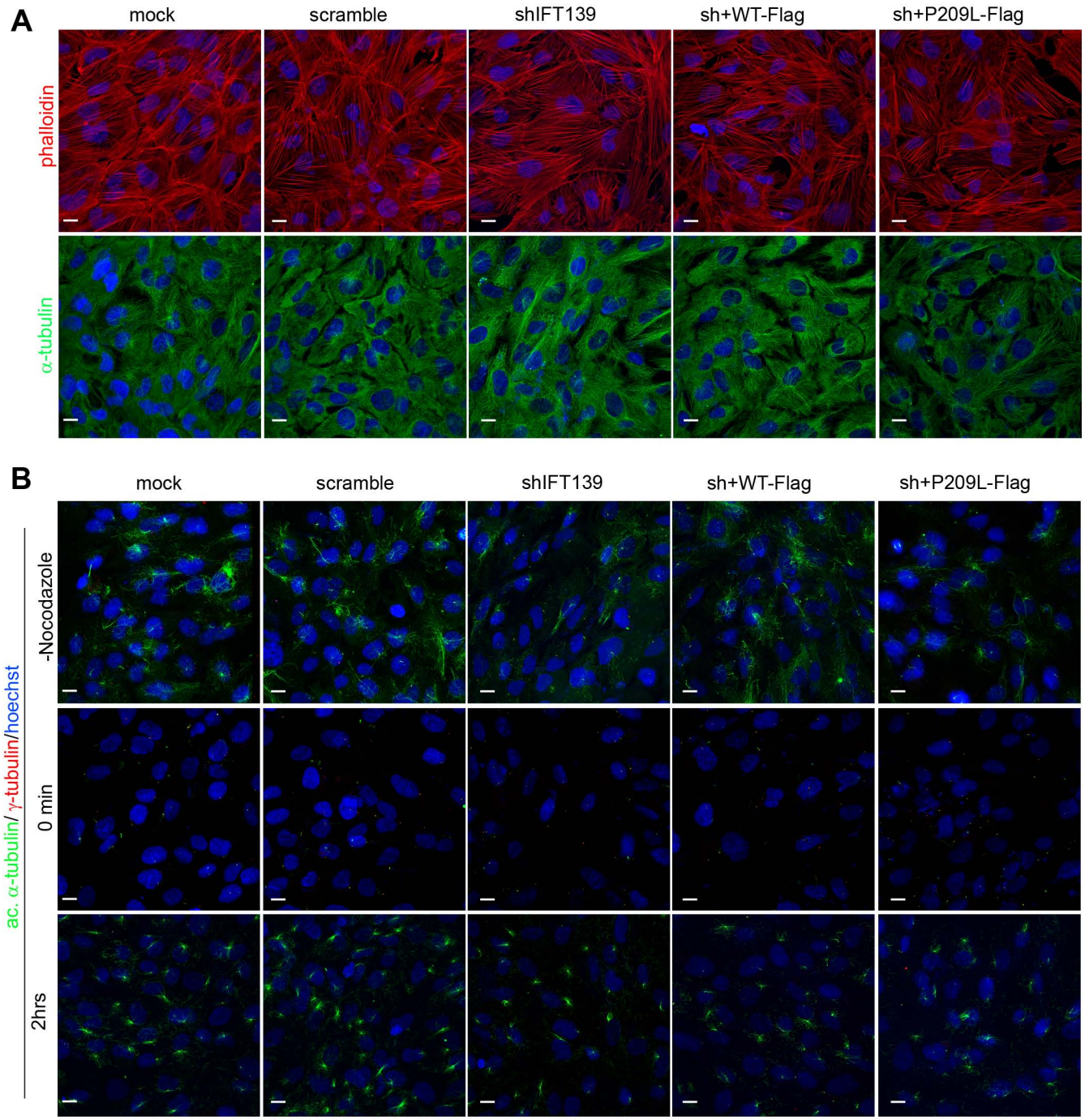

Supplemental Figure 7. (A) Phalloidin and α-tubulin staining showing respectively actin cytoskeleton and microtubules network of undifferentiated cells. Cytoskeleton defects are absent. (B) Non differentiated podocytes were treated with nocodazole for 2 hours to depolymerize microtubule network. To follow the repolymerization of tubulin cytoskeleton, cells were stained with acetylated α-tubulin in green and γ-tubulin in red. After 2 hours of recovery, we could not detect any microtubules nucleation or polymerization abnormalities in these cells. Scale bars: 20 µm.